Structures of Wild-Type Chloromet and L103N Hydroxomet *Themiste zostericola* Myohemerythrins at 1.8 Å Resolution†

Laura J. Martins,‡ Christopher P. Hill,*,§ and Walther R. Ellis, Jr.*,‡,||

Department of Chemistry, University of Utah, Salt Lake City, Utah 84112, and Department of Biochemistry, University of Utah, Salt Lake City, Utah 84132

Received December 11, 1996; Revised Manuscript Received April 7, 1997⊗

ABSTRACT: Myohemerythrin (Mhr) is a nonheme iron oxygen carrier found in the retractor muscles of marine "peanut" worms. The X-ray crystal structures of two recombinant *Themiste zostericola* Mhrs are reported to a resolution of 1.8 Å. Surprisingly, the met wild-type structure (R = 17.8%) was found to contain chloride bound to Fe2, while coordinated hydroxide was found in the met L103N structure (R = 18.3%). An internal water molecule was also found distal to the Fe−O−Fe center of the mutant protein, forming hydrogen bonds with the coordinated hydroxide and the OD1 atom of Asn-103. This finding is consistent with the kinetic and spectroscopic results reported for the L103N mutant Mhr [Raner, G. M., Martins, L. J., & Ellis, W. R., Jr. (1997) *Biochemistry 36*, 7037−7043]. Possible roles for the side chain of residue 103 (Leu in wild-type Mhr) in gating ligand binding are also discussed.

All of the presently known oxygen carriers are either iron- or copper-containing proteins (Jameson & Ibers, 1994). Beginning in the latter half of the nineteenth century, the intense colors of their respective oxy adducts prompted their isolation and characterization. Hemerythrin (Hr)[1] has been found in four phyla of marine worms and contains a diiron-oxo (Fe−O−Fe) active site. Hemocyanin, the oxygen carrier in a variety of arthropods and molluscs, also possesses a binuclear metal center, but uses copper instead of iron. Other invertebrates and vertebrates use hemoglobin, which contains a heme prosthetic group. Monomeric analogues of hemerythrin and hemoglobin, found in muscle tissue, have been designated myohemerythrin and myoglobin, respectively.

The first protein X-ray structures, which appeared in 1960, were those of sperm whale myoglobin (Figure 1; Kendrew et al., 1960) and horse hemoglobin (Perutz et al., 1960). Remarkably, neither structure revealed a channel for oxygen or other exogenous ligands to directly access the iron site from the solvent. Succeeding high-resolution structures of deoxy, oxy, and met forms of these proteins have confirmed this early observation. The lack of a "static" channel for ligand binding and release implies (Perutz, 1989) that protein fluctuations must play a key physiological role. Within the last decade, structures of a variety of hemerythrins (Sheriff et al., 1987; Holmes et al., 1991; Holmes & Stenkamp, 1991; Stenkamp, 1994) and hemocyanins (Volbeda & Hol, 1989; Hazes et al., 1993; Magnus et al., 1994) have also appeared. As indicated in Figures 1 and 2, the active sites of these proteins are binuclear. Interestingly, the metal sites of these proteins are also buried. An important consequence of this type of structural observation, often overlooked, is that ligand binding and release must involve more than one step. A key issue therefore involves the manner in which such reactions are gated in each of the three classes of O_2 carriers.

With this in mind, we have focused our attention on *Themiste zostericola* myohemerythrin (Mhr), a 13.9 kDa analogue of hemerythrin, which is found in the retractor muscles of marine "peanut" worms. Mhr possesses a four-α-helix bundle tertiary structural motif (Hendrickson et al., 1975; Kamtekar & Hecht, 1995), organized such that all four helices contribute ligands to the Fe−O−Fe core (Figure 2). Leu-103 is conserved in all of the presently known sequences (Stenkamp, 1994) of Hrs and Mhrs and lines the bottom end of a hydrophobic cavity in the interior of the four-α-helix bundle. Furthermore, the leucine methyl groups are in van der Waals contact with the exogenous ligands in the *Themiste dyscrita* oxyHr (Holmes et al., 1991), *T. dyscrita* azidometHr (Holmes & Stenkamp, 1991), and *T. zostericola* azidomet-Mhr structures (Sheriff et al., 1987). Fe1 retains its six ligands in all forms of the protein, while Fe2 can bind a variety of exogenous ligands, including dioxygen and a variety of small neutral and anionic molecules (e.g., O_2, NO, N_3^-, Cl^-). OxyMhr, produced upon binding of O_2 to diferrous deoxyMhr, is best described as a diferric hydroperoxide complex. This mode of iron−oxygen interaction is quite unusual and presently has no analogue in the coordination chemistry of simple nonheme iron complexes.

In the preceding paper in this issue (Raner et al., 1997), the kinetic and optical spectroscopic properties of three recombinant Mhrs (wild-type, L103V, and L103N) were reported. From a spectroscopic viewpoint, the gross structures of these proteins are similar. However, the L103N mutant exhibits distinctive behavior in ligand binding and redox reactions. In this report, we present the results of high-resolution (1.8 Å) X-ray structural studies of the wild-type and L103N metMhrs. Significantly, the latter contains an

† This work was supported by NIH Grants GM 43507 (W.R.E.) and GM 50163 (C.P.H.) and a grant from the Lucille P. Markey Charitable Trust (Department of Biochemistry).

* To whom correspondence should be addressed.
‡ Department of Chemistry, University of Utah.
§ Department of Biochemistry, University of Utah.
|| Present address: National Center for the Design of Molecular Function, Peterson Engineering Laboratory, Utah State University, Logan, UT 84322.

⊗ Abstract published in *Advance ACS Abstracts,* May 15, 1997.

[1] Abbreviations: Hr, hemerythrin; Mhr, myohemerythrin; SDS−PAGE, sodium dodecyl sulfate−polyacrylamide gel electrophoresis; Tris, tris(hydroxymethyl)aminomethane; PEG, poly(ethyleneglycol); rms, root mean square; σ_A, the square root of the correlation coefficient between the observed and calculated normalized structure factors.

S0006-2960(96)03042-5 CCC: $14.00

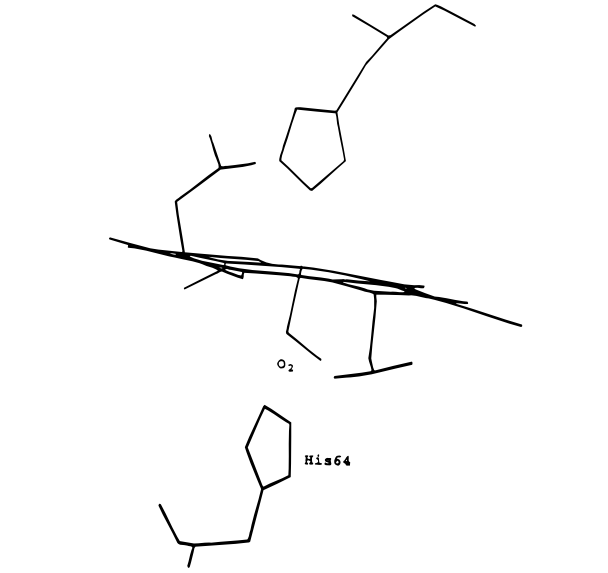

(a)

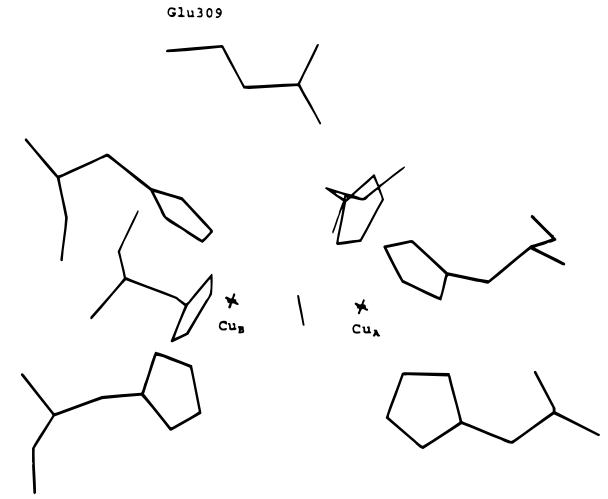

(b)

FIGURE 1: The active sites of (a) sperm whale oxymyoglobin and (b) *Lumulus polyphemus* oxyhemocyanin. Bound oxygens are displayed as bars. Distal residues that may be involved in gating are also shown.

internal water molecule hydrogen-bonded to coordinated hydroxide and the side-chain of Asn-103. Kinetic consequences, including a proposed role for Leu-103 in gating ligand binding to wild-type Mhr, also are discussed.

MATERIALS AND METHODS

Crystallization of Mhrs. The recombinant myohemerythrins used in this study were expressed in *Escherichia coli* BL-21 cells possessing either the pMHR or pL103N plasmids and purified as previously described (Raner et al., 1997). Purities of the samples for crystallization were determined to be greater than 97% by SDS−PAGE. Protein samples were dialyzed against buffer containing 0.05 M Tris-HCl, 0.2 M KCl (pH 8.0) prior to crystallization. Orthorhombic crystals sutable for X-ray diffraction studies (see Table 1 for crystal parameters) were obtained from solutions containing 27% (v/v) PEG 6K, 0.1 M HEPES, and 1.0 M LiCl (pH 7.0). These crystallization conditions differ significantly from those [0.1 M cacodylate buffer, pH 6.7, 55% $(NH_4)_2SO_4$] employed by Hendrickson and Klippenstein (1974). High-quality wild-type chlorometMhr crystals formed within 5 days at room temperature from hanging drops containing a 1:1 volume ratio of 2.16 mM protein to precipitating solution. Crystallization occurred only after removal of the denatured protein "skin" from the surfaces of the drops. L103N hydroxometMhr crystals, used for data collection, were obtained using macroseeding techniques. Small, well-formed tetragonally shaped crystals (ca. 0.01 mm) grew from solutions containing 1:1 volume ratios of 1.94 mM protein to precipitant. These crystals were washed by repeated transfers into fresh precipitating solution and then transferred into protein/precipitant solutions containing reduced protein concentrations (0.97 mM). This procedure resulted in large single crystals (ca. 1 mm). Prior to data collection, wild-type and L103N crystals were transferred into a 30% PEG 6K solution containing 1.0 M LiCl and 0.1 M HEPES, pH 7.0. No additional cryoprotectant was required for data collection at low temperature.

Data Collection. Crystals were mounted in a loop of human hair and immediately cooled in a stream of nitrogen gas (−160 °C) (Teng, 1990). X-ray diffraction data were

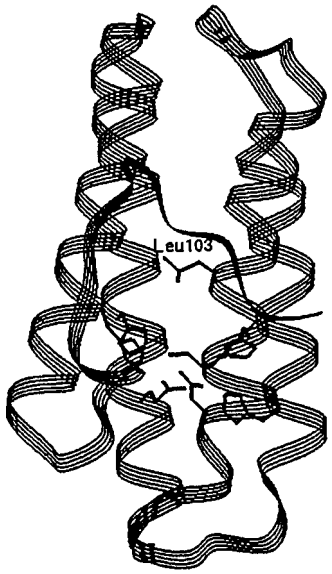

FIGURE 2: Ribbon drawing of the backbone and active-site residues of wild-type *Themiste zostericola* myohemerythrin.

Table 1: Crystallization and Data Collection Statistics

	wild-type chlorometMhr	L103N hydroxometMhr
space group	$P2_12_12_1$	$P2_12_12_1$
unit cell parameter (Å)	$a = 41.84$	$a = 41.89$
	$b = 81.26$	$b = 81.17$
	$c = 36.83$	$c = 36.69$
T (°C)	−154	−154
unique reflections	12 376	11 853
obsd reflections	91 983	102 018
R-merge[a] (%)	7.6	7.0
completeness[b] (%)	91.7 (58.3)	88.2 (49.6)

[a] R-merge $= 100\sum_{h,k,l}\sum_i|I_i - \langle I\rangle|/\sum\langle I\rangle$. [b] Values in parentheses for 1.8−1.74 Å shell. Experimental reflections were used only if $I > 1\sigma$.

collected at low temperature on an R-axis imaging plate area detector with a Rigaku RU-200 generator operating at 50 KW and 180 mA. Nearly complete data sets to 1.8 Å resolution were collected using one crystal (unit cell parameters and data collection statistics are summarized in Table 1) for each protein. Each frame consisted of either 3.2° oscillations at 30 min/frame exposure times (wild-type chlorometMhr) or 2.8° oscillations at 15 min/frame exposure (L103N hydroxometMhr). The crystal to detector distance was 130 mm with a 2θ angle of 16°. Autoindexing and data reduction were carried out using the *R*-axis software (Molecular Structure Corp.). Final $R_{merge}(I)$ values on all data were 7.6% for wild-type chlorometMhr and 7.0% for L103N hydroxometMhr. Approximately 20 reflections in each data set saturated the imaging plate. These reflections, along with reflections whose standard deviations exceeded their measured intensities, were removed from the data sets prior to refinement, resulting in removal of less than 6% of the original reflections.

Refinement. All refinement procedures were performed using the X-PLOR software package (Brünger, 1992b) on an SGI Indigo/Elan workstation. Many crystallographic calculations used programs from the CCP4 suite (CCP4, 1990). The wild-type chlorometMhr and L103N hydroxometMhr crystals were isomorphous with those of native *T. zostericola* azidometMhr crystals (Sheriff et al., 1987). The coordinates of this structure, entry number 2MHR, were obtained from the Brookhaven Protein Data Bank and used as the initial model for refinement. Solvent molecules, sulfate ions, azide, and the Fe−O−Fe moiety were removed from the starting model. In addition, disordered side chains and Leu-103, in the case of L103N hydroxometMhr, were changed to alanines (i.e., truncated) in order to reduce bias problems. A rigid body refinement was then employed using the data sets from 10.0−1.74 Å resolution, to give initial *R*-values of 48.2% and 47.2% for the wild-type chlorometMhr and L103N hydroxometMhr structures, respectively. At this stage, 10% of the data were reserved for calculation of the R^{free}-factor (Brünger, 1992a), and the refinement proceeded with rounds of simulated annealing, positional, and *B*-factor refinement, interspersed with manual map fitting using the program O (Jones et al., 1991). One round of overall *B*-factor refinement was also performed. The Fe−O−Fe moiety was positioned after the first round of automatic refinement. Side chains, previously truncated, and ordered solvent molecules/chloride ions were positioned as they became visible in $F_o - F_c$ and $2F_o - F_c$ maps. In each structure, electron density in the distal pocket was observed ca. 2.5 Å from the Fe2 atom. These features, which we have modeled as chloride and hydroxide in the wild-type chlorometMhr and L103N hydroxymetMhr structures, respectively (see Results), were left vacant (as was the distal water in the L103N structure) until the final stages of refinement, to avoid the introduction of bias into the models. In both structures, two chloride ions were found associated with the terminal nitrogens of lysines 108 and 117; their assignment as chlorides is based on *B*-values of 11−12 Å^2 (placement of waters in these positions resulted in *B*-values of only 2 Å^2). These sites are occupied by sulfate ions in the azidometMhr structure (Sheriff et al., 1987). The final *R*-factors (and free *R*-factors) are 18.1% (22.6%) and 18.7% (22.9%) for wild-type chlorometMhr and L103N hydroxymetMhr, respectively.

Table 2: Refinement Statistics

	wild-type chlorometMhr	L103N hydroxometMhr
protein non-hydrogen atoms	1183	1183
water molecules	225	205
chloride ions	3	2
R-factor[a] (%)	18.1	18.7
R^{free}-factor[b] (%)	22.6	22.9
rms deviations from ideality		
bond lengths (Å)	0.017	0.017
bond angles (deg)	2.63	2.66
average *B*-value (Å^2)		
all non-hydrogen atoms	11	13
non-hydrogen protein atoms	9	11
water molecules	20	22

[a] $R\text{-factor} = 100\sum||F_{obs}| - |F_{calc}||/\sum|F_{obs}|$. [b] The R^{free}-factor is the *R*-factor for a randomly selected subset of 10% of the data that have not been used for minimization of the crystallographic residual (Brünger, 1992a).

Target force constant values from iron−ligand (Fe−L) bond lengths and angles (L−Fe−L) are not known with high reliability. Therefore, we have minimized the possible bias due to these restraints by using low values of the force constants, which were selected to be as low as possible while consistent with maintenance of a reasonable geometry. The stereochemistries of the final structures were analyzed using the program PROCHECK (Laskowski et al., 1993). Approximately 94% of the ϕ,ψ torsion angle pairs fall within the most favored regions [the "CORE" region noted by Morris and co-workers (1992)] of Ramachandran plots for the two proteins, with the remainder in additional allowed areas. The pooled standard deviations of χ_1 for the gauche$^-$, trans, and gauche$^+$ conformers in the wild-type and L103N Mhr structures are 10.5 and 11.2°, respectively. The standard deviations in the H-bond energies are 0.64 for wild-type Mhr and 0.56 for the L103N mutant. These parameters broadly place both structures within the grouping of most reliable protein structures ("Class 1") defined by Morris and co-workers (1992). Finally, we estimate the coordinate errors, $|\Delta r|$, in the final structures, obtained by means of σ_A plots (Read, 1986), to be 0.11 and 0.15 Å for the wild-type and L103N Mhrs, respectively. The atomic coordinates and structure factors for both X-ray structures have been submitted to the Brookhaven Protein Data Bank.

RESULTS

The refinement statistics for the wild-type and mutant structures are given in Table 2. The overall structures are very similar to the *T. zostericola* azidometMhr structure, with rms deviations of atomic coordinates (excluding water molecules) less than 0.65 Å (all atoms) between all three structures. Terminal side-chain atoms of residues Lys-30, Lys-49, Lys-66, and Lys-94 diverged between the structures. This is not surprising, as lysine residues residing on protein surfaces often exhibit rotational freedom. Active-site distances are set out in Table 3.

Our low overall B-values for protein atoms, 9−11 Å^2 vs 23−24 Å^2 for azidometMhr (Sheriff et al., 1987) and metHr and azidometHr (Holmes & Stenkamp, 1991), are presumably a consequence of collecting the data at low temperature. However, the Debye−Waller factors (*B*-values) for the terminal atoms of residues Glu-3, Glu-6, Glu-23, Lys-66, Glu-82, and Lys-94 are between 25 and 35 Å^2, indicating that their positions are poorly defined.

Table 3: Active-Site Distances[a]

		distance (Å)	
atom 1	atom 2	WT chlormetMhr	L103N hydroxometMhr
Fe1	Fe2	3.26	3.24
Fe1	H73NE2	2.17	2.23
Fe1	H77NE2	2.17	2.18
Fe1	H106NE2	2.20	2.17
Fe1	E58OE1	2.09	2.11
Fe1	D111OD1	2.13	2.15
Fe1	O^{2-}	1.83	1.84
Fe2	H25NE2	2.20	2.20
Fe2	H54NE2	2.16	2.20
Fe2	E58OE2	2.14	2.13
Fe2	D111OD2	2.08	2.07
Fe2	O^{2-}	1.78	1.81
Fe2	Cl^-, OH^-	2.37	2.22

[a] The rms deviation from ideality for all bond lengths is 0.017 Å.

Electron density maps for residues surrounding the diiron-oxo clusters of the wild-type chlorometMhr and L103N hydroxo-metMhr structures are shown in Figures 3 and 4, respectively. The $2F_o - F_c$ and $F_o - F_c$ maps show that exogenous ligands are bound and complete the coordination spheres of the Fe2 atoms. It became apparent in the latter stages of refinement that the identity of this exogenous ligand differed in the wild-type and mutant structures. We have assigned these ligands as chloride (wild-type Mhr) and hydroxide (L103N Mhr) based mainly upon comparison of refined *B*-values for the ligand and the Fe−O−Fe moiety. Refinement of the wild-type metMhr exogenous ligand as chloride and the L103N metMhr exogenous ligand as hydroxide prior to two final cycles of refinement resulted in *B*-values of 7.33 and 9.0 $Å^2$, respectively. Because the L103N metMhr crystals were also grown in the presence of 1.0 M LiCl, it seemed likely that the exogenous ligand in this structure was also a chloride. However, a chloride ion at this site refined to a *B*-value of 27.9 $Å^2$ and the oxygen atom of a hydroxide ion to a *B*-value of 9.0 $Å^2$. As noted in the preceding paper in this issue (Raner et al., 1997), the electronic absorption spectrum (300−400 nm)of L103N metMhr is strongly reminiscent of a hydroxymetMhr species.

The L103N hydroxometMhr $2F_o - F_c$ and $F_o - F_c$ maps show a spherical feature between the OD1 atom of Asn-103 and the hydroxide ligand (Figure 4) that has been modeled as a water molecule. Corresponding electron density was not observed in the electron density map of wild-type chlorometMhr (Figure 3). This water molecule refined to a position 2.49 Å from the hydroxide ligand and 2.75 Å from N103OD1. The latter distance is consistent with the 2.92 ± 0.3 Å average (Jeffrey & Saenger, 1991) reported for O···O distances for water hydrogen-bonded to Asn side-chain acceptors in proteins. The *B*-value for this water molecule refined to 27.5 $Å^2$ and is higher than values obtained for other water molecules in the structure that are hydrogen bonded to two oxygen atoms, 17.7 $Å^2$, indicating that this water molecule may be disordered or partially occupied. [Firmly bound water molecules are expected (Dunitz, 1994) to have *B*-values of ca. 5−10 $Å^2$.] Figure 5 displays the superposition of the wild-type chlorometMhr and L103N

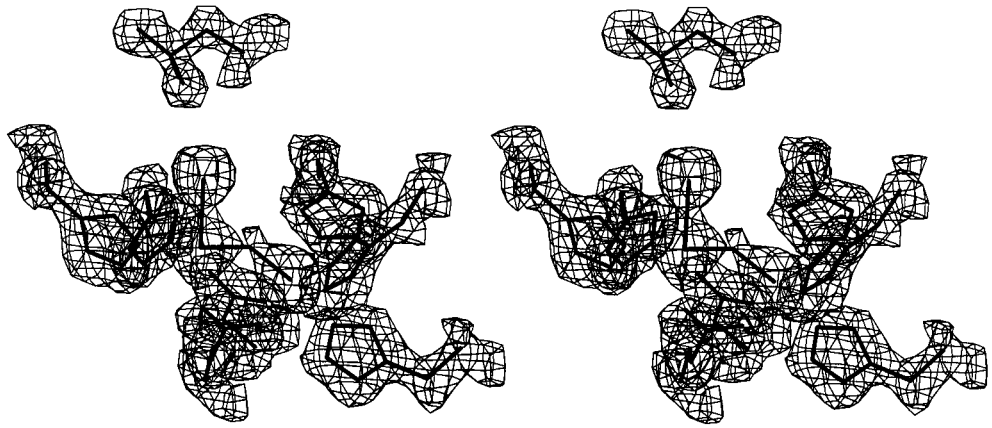

FIGURE 3: Stereo view of the electron-density map of the active site of wild-type myohemerythrin (1.2 σ contour level). Chloride is coordinated to Fe2.

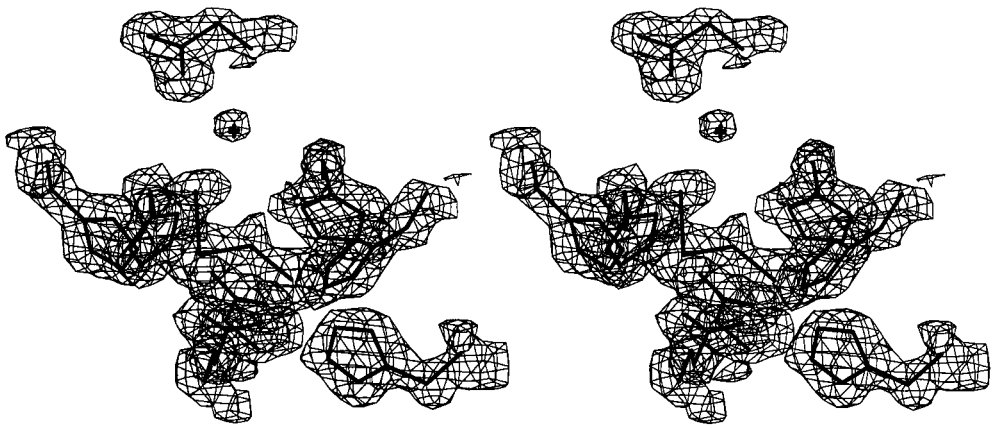

FIGURE 4: Stereo view of the electron-density map of the active site of L103N myohemerythrin (1.2 σ contour level). An internal water molecule is hydrogen-bonded to the OD1 atom of Asn-103 and coordinated hydroxide.

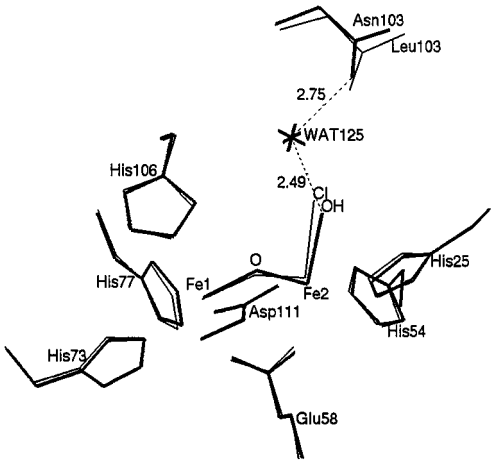

FIGURE 5: Superposition of the active-site structures of the wild-type chlorometand L103N hydroxomet myohemerythrins.

hydroxometMhr structures in the vicinity of the Fe−O−Fe center.

DISCUSSION

Overexpressed wild-type and L103N Mhrs were observed to appear in the soluble and insoluble portions of *E. coli* cell extracts (Raner et al., 1997). Further characterization indicated that the L103N mutant was only produced as the apoprotein, requiring subsequent *in vitro* reconstitution with iron. Despite the failure of the L103N Mhr to properly fold and form an Fe−O−Fe center *in vivo*, the wild-type and L103N structures are very similar to each other. In particular, the Fe1−Fe2 distances (Table 3) and Fe−O−Fe angles (129 ± 3° and 126 ± 3° for wild-type chlorometMhr and L103N hydroxometMhr, respectively) are in good agreement with those reported for azidometMhr (Sheriff et al., 1987) and azidometHr (Holmes & Stenkamp, 1991). Furthermore, ligation of Fe2 by azide, chloride, and hydroxide all result in similar Fe−O(bridge) distances, ca. 1.8 Å.

The structures reported here differ in the anion coordinated to Fe2, even though crystals of the wild-type and L103N Mhrs were prepared from solutions containing identical buffer, LiCl and PEG compositions. In support of our assignments of the anion identities, we note that the electronic absorption spectrum of the recombinant wild-type metMhr in the presence of 1.0 M LiCl is similar to that of chlorometHr (Garbett et al., 1969; Reem et al., 1989). The wild-type metMhr spectrum is also pH independent, suggesting that hydroxide does not ligate to this protein. In contrast, the absorption spectrum of L103N metMhr is unperturbed upon addition of LiCl to a concentration of 1.0 M (Sanders-Loehr, J., unpublished results). The L103N electron density map (Figure 4) clearly shows an additional feature, modeled as a water molecule, within hydrogen-bonding distance of the coordinated hydroxide and the N103OD1 atom. This interaction is in contrast to one, involving a hydrogen bond between coordinated hydroxide and the bridging oxygen, suggested (Shiemke et al., 1986) to occur at low temperature on the basis of the temperature dependence of the resonance Raman spectrum of *Phascolopsis gouldii* hydroxometHr.

The distal water molecule in the L103N structure is presumably responsible for the different anions coordinated to Fe2 in the two structures presented herein. The fact that hydroxide is the preferred ligand, even in 1.0 M LiCl, suggests that a hydrogen-bonding interaction with the water in the distal cavity may destabilize other potential ligands capable of being protonated (e.g., Cl^-). Raner and co-workers (1997) observed azide binding constants (25 °C, pH 8.0) of 2.3×10^5 M^{-1} and 500 M^{-1}, respectively, for wild-type and L103N Mhrs. We also note that our attempts to prepare L103N azidometMhr crystals for X-ray analysis failed because infusion of sodium azide shattered the L103N hydroxometMhr crystals. To the best of our knowledge, this effect of an internal water molecule on ligand binding is the most extreme observed to date for any metalloprotein. It is interesting to note, however, that a water molecule was located within hydrogen-bonding distance of the bridging μ-oxo group in the structure of *T. dyscrita* metHr (Holmes & Stenkamp, 1991), which contains a five-coordinate Fe2 center (i.e., there is no exogenous ligand). Of related interest, Quiocho and co-workers (1989) have noted that ordered water can markedly influence the binding of carbohydrates by the L-arabinose-binding protein.

It is likely that the distal water molecule is also present in the room-temperature structure as well. The kinetics of azide binding to the L103N hydroxometMhr were observed (Raner et al., 1997) to be a factor of 6 slower than for the wild-type metMhr, suggesting that the distal region of the L103N mutant is occupied by species (hydroxide and water) that must be expelled by azide to form the azidomet analogue. Oxygen reacts with L103N deoxyMhr to produce an oxy adduct that rapidly autoxidizes, resulting in hydroxometMhr and released hydrogen peroxide. It therefore appears that a rather hydrophobic environment is needed to stabilize the oxy adduct of Mhr. This will make the synthesis of an accurate, functional Mhr model complex difficult indeed.

Two brachiopod Hrs (Manwell, 1960; Richardson et al., 1983; Zhang & Kurtz, 1991) consist of $\alpha_4\beta_4$ octamers that display cooperative oxygen uptake. A resonance Raman study (Kaminaka et al., 1992) of one of these noted a pH-dependent shift of the ν_{O-O} stretch of the oxy form. This was interpreted in terms of a hydrogen-bonding interaction, between bound dioxygen and an unidentified amino acid, that acts to stabilize the higher-affinity oxy structure. In view of the structural and kinetic observations for L103N Mhr, it seems that such a hydrogen bond would destabilize the Hr oxy adduct. More likely, a slight movement of the Leu-103 side chain vis-à-vis bound dioxygen, which may regulate the strength of the hydrogen bond between the hydroperoxide (bound O_2) and the oxo bridge, or a pH-dependent movement of one of the endogenous iron ligands is responsible for the observed Raman spectral shift.

As noted in the beginning of this paper, refined X-ray structures are presently available for representatives of all three families of O_2 carriers. Interestingly, the active sites are buried in all of the structures, indicating that protein fluctuations are required in order for O_2 and other exogenous ligands to coordinate to a metal in these proteins. Crystallographic (Perutz, 1989) and mutagenesis (Olson et al., 1988) work point to a role for the distal histidine in gating ligand binding to most myoglobins and hemoglobins. (Asian elephant myoglobin contains a distal glutamine.) Hazes and co-workers (1993) similarly suggested that Glu-309 blocks access the the dicopper site in hemocyanin. We propose that Leu-103 plays a analogous role in the hemerythrins and myohemerythrins. As illustrated in Figure 6, Fe2 can be

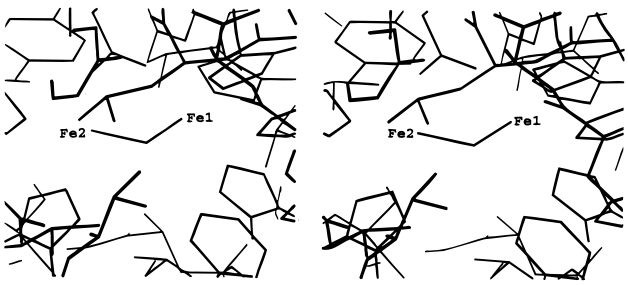

FIGURE 6: View of the interhelical cavity of myohemerythrin, indicating that the position of the Leu-103 side chain blocks access to Fe2. Rotation about the $C_\alpha-C_\beta$ bond would open up a channel for ligand access to Fe2.

accessed by exogenous ligands from the hydrophobic core. Anion binding to Hr and Mhr has been shown (Meloon & Wilkins, 1976) to be accelerated by lower pH, consistent with their entry into the core as protonated species. Regardless of the manner in which structural fluctuations in O_2 carriers occur, the fact that X-ray structural studies consistently show that the metal sites are not directly accessible by exogenous ligands demonstrates that single-step equilibrium kinetic models (e.g., O_2 + deoxyprotein $\rightleftarrows$ oxyprotein) for ligand binding and release cannot be correct. In particular, recent work (Lloyd et al., 1995; Yedgar et al., 1995) demonstrates that the mechanism (DeWaal & Wilkins, 1976; Petrou et al., 1981; Armstrong & Sykes, 1986) of O_2 uptake and release by Hr and Mhr must be reconsidered.

ACKNOWLEDGMENT

We thank David Worthylake and Felix Vajdas for helpful assistance with the use of computer programs.

REFERENCES

Armstrong, G. D., & Sykes, A. G. (1986) *Inorg. Chem. 25*, 3135−3139.
Brünger, A. T. (1992a) *Nature 355*, 472−475.
Brünger, A. T. (1992b) *X-PLOR: A System for Crystallography and NMR*, Yale University Press, New Haven, CT.
Collaborative Computing Project 4 (1990) *J. Appl. Crystallogr. 23*, 387−391.
DeWaal, D. J. A., & Wilkins, R. G. (1976) *J. Biol. Chem. 251*, 2339−2346.
Dunitz, J. D. (1994) *Science 264*, 670.
Garbett, K.; Darnall, D. W.; Klotz, I. M.; Williams, R. J. P. (1969) *Arch. Biochem. Biophys. 135*, 419−434.
Hazes, B., Magnus, K. A., Bonaventura, C., Bonaventura, J., Dauter, Z., Kalk, K. H., & Hol, W. G. J. (1993) *Protein Sci. 2*, 597−619.
Hendrickson, W. A., & Klippenstein, G. L. (1974) *J. Mol. Biol. 87*, 147−149.
Hendrickson, W. A., Klippenstein, G. L., & Ward, K. B. (1975) *Proc. Natl. Acad. Sci. U.S.A. 72*, 2160−2164.
Holmes, M. A., & Stenkamp, R. E. (1991) *J. Mol. Biol. 220*, 723−737.
Holmes, M. A., Le Trong, I., Turley, S., Sieker, L. C., & Stenkamp, R. E. (1991) *J. Mol. Biol. 218*, 583−593.
Jameson, G. B., & Ibers, J. I. (1994) in *Bioinorganic Chemistry* (Bertini, I., Gray, H. B., Lippard, S. J., & Valentine, J. S., Eds.) pp 167−252, University Science Press, Mill Valley, CA.
Jeffrey, G. A., & Saenger, W. (1991) *Hydrogen Bonding in Biological Structures*, p 476, Springer-Verlag, New York.
Jones, T. A., Zou, J. Y., Cowan, S. W., & Kjeldgaard, M. (1991) *Acta Crystallogr. A47*, 110−119.
Kaminaka, S., Takizawa, H., Handa, T., Kihara, H., & Kitagawa, T. (1992) *Biochemistry 31*, 6997−7002.
Kamtekar, S., & Hecht, M. H. (1995) *FASEB J. 9*, 1013−1022.
Kendrew, J. C., Dickerson, R. E., Strandberg, B. E., Hart, R. G., Davies, D. R., Phillips, D. C., & Shore, V. C. (1960) *Nature 185*, 422−427.
Laskowski, R. A., MacArthur, M. W., Moss, D. S., & Thornton, J. M. (1993) *J. Appl. Crystallogr. 26*, 283−291.
Lloyd, C. M., Eyring, E. M., & Ellis, W. R., Jr. (1995) *J. Am. Chem. Soc. 117*, 11993−11994.
Magnus, K. A., Ton-That, H., & Carpenter, J. E. (1994) *Chem. Rev. 94*, 727−735.
Manwell, C. (1960) *Science 132*, 550−551.
Meloon, D. R., & Wilkins, R. G. (1976) *Biochemistry 15*, 1284−1290.
Morris, A. C., MacArthur, M. W., Hutchinson E. G., & Thornton, J. M. (1992) *Proteins 12*, 345−364.
Olson, J. S., Mathews, A. J., Rohlfs, R. J., Springer, B. A., Egeberg, K. D., Sligar, S. G., Tame, J., Renaud, J.-P., & Nagai, K. (1988) *Nature 336*, 265−266.
Perutz, M. F. (1989) *Trends Biochem. Sci. 14*, 42−44.
Perutz, M. F., Rossmann, M. G., Cullis, A. F., Muirhead, H., Will, G., & North, A. C. T. (1960) *Nature 185*, 416−422.
Petrou, A. L., Armstrong, F. A., Sykes, A. G., Harrington, P. C., & Wilkins, R. G. (1981) *Biochim. Biophys. Acta 670*, 377−384.
Quiocho, F. A., Wilson, D. K., & Vyas, N. K. (1989) *Nature 340*, 404−407.
Raner, G. M., Martins, L. J., & Ellis, W. R., Jr. (1997) *Biochemistry 36*, 7037−7043.
Read, R. J. (1986) *Acta Crystallogr. A42*, 140−149.
Reem, R. C.; McCormick, J. M.; Richardson, D. E.; Devlin, F. J.; Stephens, P. J.; Musselman, R. L.; Solomon, E. I. (1989) *J. Am. Chem. Soc.* 111, 4688−4704.
Richardson, D. E., Emad, M., Reem, R. C., & Solomon, E. I. (1987) *Biochemistry 26*, 1003−1013.
Sheriff, S., Hendrickson, W. A., & Smith, J. L. (1987) *J. Mol. Biol. 197*, 273−296.
Shiemke, A. K., Loehr, T. M., & Sanders-Loehr, J. (1986) *J. Am. Chem. Soc. 108*, 2437−2443.
Stenkamp, R. E. (1994) *Chem. Rev. 94*, 715−726.
Stenkamp, R. E., Sieker, L. C., Jensen, L. H., McCallum, J. D., & Sanders-Loehr, J. (1985) *Proc. Natl. Acad. Sci. U.S.A. 82*, 713−716.
Teng, T.-Y. (1990) *J. Appl. Crystallogr. 23*, 387−391.
Volbeda, A., & Hol, W. G. J. (1989) *J. Mol. Biol. 209*, 249−279.
Yedgar, S., Tetreau, C., Gavish, B., & Lavalette, D. (1995) *Biophys. J. 68*, 665−670.
Zhang, J. H., & Kurtz, D. M., Jr. (1991) *Biochemistry 30*, 9121−9125.

BI9630422